

Raman spectroscopy of walpurgite

Ray L. Frost ^{a*}, Matt L. Weier ^a, Jiří Čejka ^b and J. Theo Kloprogge ^a

^a Inorganic Materials Research Program, School of Physical and Chemical Sciences, Queensland University of Technology, GPO Box 2434, Brisbane Queensland 4001, Australia.

^b National Museum, Václavské náměstí 68, CZ-115 79 Praha 1, Czech Republic.

This is the authors' version of a paper published as:

Frost, R. Čejka, J. Weier, M. & Kloprogge, T. (2006) Raman spectroscopy of walpurgite. *Journal of Raman Spectroscopy* 37(5):pp. 585-590.
Copyright 2006 John Wiley & Sons

Abstract

Raman spectra of walpurgite, $(\text{UO}_2)\text{Bi}_4\text{O}_4(\text{AsO}_4)_2 \cdot 2\text{H}_2\text{O}$, recorded at 298 K and 77 K are presented and compared with infrared spectra of walpurgite and phosphowalpurgite. Bands connected with $(\text{UO}_2)^{2+}$, $(\text{AsO}_4)^{3-}$ and H_2O stretch and bend, and Bi-O stretch are tentatively assigned. Hydrogen bond lengths are calculated from the wavenumbers of the H_2O stretching vibrations and compared with those from crystal structure analysis of walpurgite.

Keywords: walpurgite, mineral, Bi_4O_4 , uranyl, arsenate, molecular water, hydrogen bonds, Raman spectroscopy

Introduction

Walpurgite is a rare secondary mineral of formula $(\text{UO}_2)\text{Bi}_4\text{O}_4(\text{AsO}_4)_2 \cdot 2\text{H}_2\text{O}$ ^{1,2}. It is a hydrated bismuth uranyl arsenate oxide of high density 5.95 to 6.9. The mineral is often associated with other uranium minerals including bismutite, torbernite, zeunerite, uraninite and other uranium minerals. The mineral is related to orthowalpurgite and the phosphate analogue phosphowalpurgite³⁻⁵. The mineral is triclinic and is of space group P1 (no. 2)^{2,5,6}. Orthowalpurgite (space group Pbcm, no. 57) is a polymorph of walpurgite⁵ and there is also one phosphate analogue⁵. The mineral is translucent to transparent with the colour straw yellow to colourless. From the topology point of view, Burns⁷ classifies walpurgite and orthowalpurgite as structures based upon infinite chains. According to Burns⁷ and Burns et al.⁸, the crystal structures of walpurgite⁸ and orthowalpurgite⁵ are based on the chain which contains UO_2O_4 square dipyramids and AsO_4 tetrahedra. Each UO_2O_4 square dipyramid shares all four corners with AsO_4 tetrahedra that provide the linkages between adjacent uranyl polyhedra along the chain length. The uranyl ions of the UO_2O_4 square dipyramids are oriented roughly perpendicular to the chain length. The structures of both orthowalpurgite and walpurgite contain two symmetrically distinct Bi polyhedra, which are coordinated by six or seven ligands. The BiO_n polyhedra link to form sheets that are in turn linked by the uranyl arsenate chains. Burns⁷ points out

* Author to whom correspondence should be addressed (r.frost@qut.edu.au)

that the structures of walpurgite and orthowalpurkite are evidently polymorphs, and differ mainly in the alignment of adjacent uranyl arsenate chains. Only infrared spectra of walpurgite are available^{3,4,9}.

The aim of this paper is to present Raman spectra of walpurgite recorded at 298 K and 77 K and to compare these spectra with published infrared spectra of walpurgite, phosphatian walpurgite and phosphowalpurkite^{3,4}. Raman spectra of walpurgite are published for the first time.

Experimental

Mineral

The mineral walpurgite was obtained from The Australian Museum and is a standard reference mineral. The mineral originated from Weisser Hirsch Mine, Schneeberg, Saxony, Germany. The mineral was analysed by EDX methods for chemical composition. Some phosphate at levels ~1% was determined. The phosphate dominant mineral is termed phosphowalpurkite.

Raman spectroscopy

The crystals of walpurgite were placed on the stage of an Olympus BHSM microscope, equipped with 10x and 50x objectives and part of a Renishaw 1000 Raman microscope system, which also includes a monochromator, a filter system and a Charge Coupled Device (CCD). Raman spectra were excited by a HeNe laser (633 nm) at a resolution of 2 cm⁻¹ in the range between 100 and 4000 cm⁻¹. Repeated acquisition using the highest magnification was accumulated to improve the signal to noise ratio. Spectra were calibrated using the 520.5 cm⁻¹ line of a silicon wafer. In order to ensure that the correct spectra are obtained, the polarization of the incident excitation radiation was scrambled. Previous studies by the authors provide more details of the experimental technique. Spectra at liquid nitrogen temperature were obtained using a Linkam thermal stage (Scientific Instruments Ltd, Waterfield, Surrey, England). Details of the technique have been published by the authors elsewhere¹⁰⁻¹³.

Results and Discussion

Walpurgite is an unusual mineral in its formulation as it contains not only uranyl groups but arsenate and bismuth oxide units. Thus the spectroscopy of this mineral will be made up of the spectroscopy of the subunits. The D_{∞h} symmetry of the free uranyl, (UO₂)²⁺, and T_d symmetry of the (AsO₄)³⁻ groups are lowered causing infrared and Raman activation of all (UO₂)²⁺ and (AsO₄)³⁻ vibrations and splitting of doubly and triply degenerate vibrations in the spectra of walpurgite. The factor group analysis of the uranyl, arsenate and water units are given in Tables 1-3 respectively. The irreducible representation is given by $\Gamma = 24A_u + 26A_g$. There are 28 internal vibrations and 50 lattice vibrations giving a total of 78 predicted vibrations. For walpurgite N=27 [Bi₄ (UO₂) (AsO₄)₂ O₄ 2H₂O] hence 3n-3 = 3*27-2 = 78. Only one symmetrically distinct uranyl group and one symmetrically distinct arsenate group and two symmetrically distinct Bi atoms are present in the crystal structure of walpurgite (Z = 1)⁹. According to Hawthorne¹⁴⁻¹⁶ from the general point of view, and the conclusions by Burns concerning uranium minerals, hydrogen bonding is of

fundamental importance to the stability of the structure of minerals. Burns ⁷ and Burns et al. ^{8,17} also proposed hydrogen bonding network in the crystal structures on the basis of crystal-chemical and bond-valence parameters arguments. This may be applied also to walpurgite. Thus tentative assignment of the bands observed is therefore made with regard to all these assumptions.

Figure 1 displays the Raman spectra at 298 and 77 K of walpurgite in the 650 to 950 cm^{-1} region. The results of the Raman spectral analysis are reported in Table 1. This table also draws a comparison with previously published infrared data ³⁻⁵. No Raman spectra of these mineral types have been published. Two distinct sets of bands are observed centred upon 836 and 790 cm^{-1} . A problem exists as to the assignment of these bands. The bands may be assigned to either the $(\text{AsO}_4)^{3-}$ units or the $(\text{UO}_2)^{2+}$ units. The first band may be assigned to the symmetric stretching mode of the $(\text{AsO}_4)^{3-}$ units. The band at 836.4 cm^{-1} shifts to 838.6 cm^{-1} with a significantly reduced band width at 77 K. Infrared bands were not obtained as the mineral sample was on loan. Alternatively this band may be assigned to the symmetric stretching mode of the $(\text{UO}_2)^{2+}$ units. Bands at 857.4, 836.4 and 822.7 cm^{-1} may be also attributed to the split triply degenerate ν_3 $(\text{AsO}_4)^{3-}$ antisymmetric stretching vibrations. Previous studies by the authors have suggested bands at around 836 cm^{-1} are due to the ν_3 antisymmetric stretching modes of the $(\text{AsO}_4)^{3-}$ units ¹⁸⁻²³. The assignment of bands differs from that published by Sejkora et al. based upon empirical calculations, it was estimated that the bands between 806 and 837 cm^{-1} are assignable to the ν_1 symmetric stretching mode of $(\text{UO}_2)^{2+}$ units ³. Of course it is possible that an overlap or coincidence between the symmetric stretching modes of $(\text{UO}_2)^{2+}$ units and the ν_1 symmetric stretching modes of the $(\text{AsO}_4)^{3-}$ units or even the split triply degenerate ν_3 antisymmetric stretching modes of the $(\text{AsO}_4)^{3-}$ units cannot be ruled out. U-O bond lengths in uranyl, calculated with empirical relation by Bartlett and Cooney ²⁴ using wavenumbers 799 and 838 cm^{-1} of the two bands which may be attributed to the ν_1 $(\text{UO}_2)^{2+}$, correspond to 1.812 and 1.773 Å, respectively. These values are comparable with 1.784 Å for walpurgite [24] and differ from the average value 1.91 Å for orthowalpurgite ^{3,4}, inferred from single crystal structure analysis of both minerals.

Low intensity bands are observed at 850 and 892 cm^{-1} . This latter band is assigned to the ν_3 antisymmetric stretching mode of $(\text{UO}_2)^{2+}$ units. The band is observed at 889.3 cm^{-1} in the 77K spectrum. This value fits well with published infrared data. Infrared absorption bands have been observed for phosphowalpurgite at 885 cm^{-1} and at 888 cm^{-1} for walpurgite. These bands have been assigned to the antisymmetric stretching ν_3 vibrations of the $(\text{UO}_2)^{2+}$ units ³. Bands close to 1003, 948.2, 546 and 430 cm^{-1} may be assigned to the stretching and bending vibrations of $(\text{PO}_4)^{3-}$ units which partly substitute $(\text{AsO}_4)^{3-}$ units in the structure of walpurgite ^{3,4}.

The set of bands centred upon 790.1 cm^{-1} are assigned to the $(\text{UO}_2)^{2+}$ symmetric stretching vibrations. Two bands are found at 790.1 and 770.9 cm^{-1} . The 298 K spectral profile may be resolved into bands at 796.5, 786.6 and 771.3 cm^{-1} in the 77 K spectrum. The observation of multiple bands in this region may well correspond with the non-equivalence of the UO bonds. This assignment differs from published data based upon the infrared spectrum of walpurgite and phosphowalpurgite ^{3,4}. In table 3 of the reference on phosphowalpurgite strong infrared bands were given

at 778 cm^{-1} but were assigned to $(\text{AsO}_4)^{3-}$ - ν_1 symmetric stretching modes. The arsenate analysis of the phosphowalpurkite gave a weight % of 3.47 to 5.73 %. The phosphate analysis ranged from 6.73 to 8.8 %. Hot stage Raman spectroscopy of metazeunerite showed bands at 811 and 790 cm^{-1} that were assignable to $(\text{UO}_2)^{2+}$ stretching vibrations²⁵. In this example no Raman spectra of the $(\text{AsO}_4)^{3-}$ units were observed until after the thermal decomposition. However, it should be noted, that, according to single crystal structure analysis of walpurkite²⁶, only one symmetrically distinct uranyl is present in the structure, and the U-O bond lengths in uranyl are practically of the same value $\{1.784(14)\text{ \AA}\}$. Intense bands at 770 - 771 cm^{-1} may be alternatively also attributed to the Raman active ν_1 $(\text{AsO}_4)^{3-}$ symmetric stretching vibrations.

The Raman spectrum of the low wavenumber region of walpurkite is displayed in Figure 2. A very sharp and intense band is observed at 513.3 cm^{-1} (298 K) and at 516.9 cm^{-1} (77 K). One possible assignment of this band is to the BiO stretching vibration as no $(\text{UO}_2)^{2+}$ and $(\text{AsO}_4)^{3-}$ bands are found in this spectral region. Previous infrared studies gave an intense band at 524 or 534 cm^{-1} . This band was assigned to BiO or BiOBi stretching vibrations^{3,4}. Calculations would suggest that the first assignment is the most likely vibration. Two bands are observed in the low wavenumber region at 491.4 and 431.9 cm^{-1} . These two bands are assigned to the ν_4 $(\text{AsO}_4)^{3-}$ bending vibrations. Infrared bands were observed for walpurkite at 432 cm^{-1} and were ascribed to ν_4 $(\text{AsO}_4)^{3-}$ bending modes. Two bands are observed at 376.7 and 333.5 cm^{-1} . Bands in these positions may be due to the ν_2 $(\text{AsO}_4)^{3-}$ bending vibrations. An intense band is found at 295.9 cm^{-1} in the 298 K spectrum. This band is assigned to the $(\text{UO}_2)^{2+}$ bending modes. The band shifts to 299 cm^{-1} at 77K. Another band observed at lower wavenumber (277.8 or 239.9 cm^{-1}) may be also connected and therefore attributed to the split to the ν_2 (δ) $(\text{UO}_2)^{2+}$ bending vibration. The other bands in the wavenumber region lower than 300 cm^{-1} may be attributed to the lattice vibrations. Bands in the region from 614 to 721 cm^{-1} may be assigned to H_2O libration modes, and that at 1323 cm^{-1} (298 K) may be attributed to an overtone or a combination band.

The Raman spectrum of the hydroxyl stretching region of walpurkite between 3200 and 3400 cm^{-1} is shown in Figure 3. The spectrum is not of good quality (lack of signal to noise) but two bands are observed at 3515.8 and 3375.6 cm^{-1} . These bands are attributed to the water antisymmetric and symmetric stretching modes. The position of the bands suggests that significant hydrogen bonding exists in the walpurkite structure. The crystal structure of walpurkite shows that there are two distinct water molecules in the unit cell²⁶. These water molecules may not necessarily be explicitly symmetrically distinct but there is the possibility that the two water molecules are not equivalent. If we use a Libowitzky type empirical equation²⁷, and we assume that we can use Raman data in the equation, estimates of the hydrogen bond distances can be obtained. The values for the OH stretching vibrations give calculated hydrogen bond distances of 2.920 and 2.782 \AA . Thus two water molecules with different hydrogen bond distances are found in the walpurkite structure. One hydrogen bond is shorter than the second hydrogen bond. Spectra were obtained at 77 K but the signal to noise ratio was less than is required for such calculations. This conclusion is supported by the fact that two hydrogen bonds O-H...O with lengths 2.77 and 2.88 \AA were inferred from the single crystal structure analysis of walpurkite²⁶.

It is unusual to observe water bending modes in Raman spectroscopy. Water is a very poor Raman scatterer and the band is more readily identified with infrared spectroscopy. Nevertheless the presence of water is identified by a band centred at 1597 cm^{-1} (Figure 4). Bands in this position are indicative of non-hydrogen bonded or weakly hydrogen bonded water molecules. Bands for water vapour are found in these positions. The band at 1325 cm^{-1} may be assigned to uranyl OH deformation mode. (Figure 4). In secondary minerals containing the uranyl and water units, it is possible that some dissociation of the water molecules occurs into hydrogen ions and hydroxyl ions. Thus the possibility is that there are some OH units in the structure and that this band is a uranyl OH deformation is real. The band is of low intensity and has poor signal to noise. The band if the assignment is correct brings into question the exact formula of walpurgite.

Conclusions

Walpurgite is a secondary uranyl mineral, known for many years, containing $(\text{UO}_2)^{2+}$, (Bi_4O_4) , $(\text{AsO}_4)^{3-}$ and molecular water. Its crystal structure is known. However, this paper proves that Raman spectroscopy corroborates and extends knowledge of such natural phases. Observed bands were tentatively assigned to the vibrations of $(\text{UO}_2)^{2+}$, (BiO) and $(\text{AsO}_4)^{3-}$ units and water molecules. Some coincidences of bands in the region of stretching and bending vibrations of these units cannot be excluded. H-bond lengths were inferred from the wavenumbers of bands assigned to the molecular water stretching vibrations.

Acknowledgements

The financial and infra-structure support of the Queensland University of Technology Inorganic Materials Research Program of the School of Physical and Chemical Sciences is gratefully acknowledged. The Australian Research Council (ARC) is thanked for funding.

Mr Ross Pogson of The Australian Museum is thanked for the supply of the walpurgite mineral.

References

1. Fischer, E. *Neues Jahrb. Mineral., Geol., Monatsh.* 1948; **A**: 44.
2. Fischer, E. *Zeitschrift fuer Kristallographie, Kristallgeometrie, Kristallphysik, Kristallchemie* 1945; **106**: 25.
3. Sejkora, J, Cejka, J, Hlousek, J, Novak, M, Srein, V. *Canadian Mineralogist* 2004; **42**: 963.
4. Sejkora, J, Cejka, J, Hlousek, J, Srein, V, Novotna, M. *Neues Jahrbuch fuer Mineralogie, Monatshefte* 2002: 353.
5. Krause, W, Effenberger, H, Brandstaetter, F. *European Journal of Mineralogy* 1995; **7**: 1313.
6. Braithwaite, RSW, Knight, JR. *Mineralogical Magazine* 1990; **54**: 129.
7. Burns, PC. *Reviews in Mineralogy* 1999; **38**: 23.
8. Burns, PC, Miller, ML, Ewing, RC. *Canadian Mineralogist* 1996; **34**: 845.
9. Cejka, J. *Reviews in Mineralogy* 1999; **38**: 521.
10. Frost, RL, Weier, ML. *Thermochimica Acta* 2003; **406**: 221.
11. Frost, RL, Weier, ML, Kloprogge, JT. *Journal of Raman Spectroscopy* 2003; **34**: 760.
12. Frost, RL, Weier, ML. *Journal of Raman Spectroscopy* 2003; **34**: 776.
13. Frost, RL, Weier, ML. *Thermochimica Acta* 2004; **409**: 79.
14. Hawthorne, FC. *Zeitschrift fuer Kristallographie* 1992; **201**: 183.
15. Hawthorne, FC. *EMU Notes in Mineralogy I* 1997; **European Mineralogical Union**: 373.
16. Hawthorne, FC. *Acta Crystallographica, Section B: Structural Science* 1994; **B50**: 481.
17. Burns, PC, Ewing, RC, Hawthorne, FC. *Canadian Mineralogist* 1997; **35**: 1551.
18. Frost, RL, Martens, WN, Williams, PA. *Journal of Raman Spectroscopy* 2002; **33**: 475.
19. Frost, RL, Martens, W, Williams, PA, Kloprogge, JT. *Journal of Raman Spectroscopy* 2003; **34**: 751.
20. Frost, RL, Kloprogge, JT, Martens, WN. *Journal of Raman Spectroscopy* 2004; **35**: 28.
21. Martens, W, Frost, RL, Kloprogge, JT. *Journal of Raman Spectroscopy* 2003; **34**: 90.
22. Martens, W, Frost, RL, Williams, PA. *Journal of Raman Spectroscopy* 2003; **34**: 104.
23. Martens, WN, Kloprogge, JT, Frost, RL, Rintoul, L. *Journal of Raman Spectroscopy* 2004; **35**: 208.
24. Bartlett, JR, Cooney, RP. *Journal of Molecular Structure* 1989; **193**: 295.
25. Frost, RL, Weier, ML, Adebajo, MO. *Thermochimica Acta* 2004; **419**: 119.
26. Mereiter, K. *TMPM, Tschermarks Mineralogische und Petrographische Mitteilungen* 1982; **30**: 129.
27. Libowitzky, E. *Monatshefte fuer Chemie* 1999; **130**: 1047.
28. Sejkora, J, Veselovsky, F, Srein, V. *Acta Musei Nationalis Pragae, Ser. B, Hist. Natur.* 1994; **B50**: 55.

Table 1 Factor group Analysis of the $(\text{UO}_2)^{2+}$ vibrations

$D_{\infty h}$	C_i	C_i
Σ_g^+	A_g	A_g
Σ_u^+ Π_u	$3A_u$	$3A_u$

Table 2 Factor group Analysis of the $(\text{AsO}_4)^{3-}$ vibrations

T_d	C_1	C_i
A_1		$9A_g$
E	$9A$	
$2T_2$		$9A_u$

Table 3 Factor group Analysis of the H_2O vibrations

C_{2v}	C_1	C_i
$2A_1$	$3A$	$3A_g$
B_2		$3A_u$

Walpurgite Raman spectra						Phospho Walpurgite 3	Phospho Walpurgite 4	Walpurgite 28	
298K Raman			77K Raman			Infrared	Infrared	Infrared	Assignments
Center cm ⁻¹	FWH M cm ⁻¹	Area %	Center cm ⁻¹	FWH M cm ⁻¹	Area %	Center cm ⁻¹	Center cm ⁻¹	Center cm ⁻¹	
3515	116.8	1.0						3520	Water OH stretching vibrations
3375	152.1	1.3	3320.4	53.4	0.9	3442	3449	3380	Water OH stretching vibrations
						2928	2934		
						2862	2862		
1597	82.5	1.9				1630	1634	1604	Water bending modes
						1463			
						1387	1390		
1323	124.9	2.0				1271	1274		OH deformation
						1150	1152		
1003	49.9	1.3				1035	1027	1028	Phosphate antisymmetric stretching
						998	1000		
						969	964		Sulphate symmetric stretching??
948.2	27.3	0.6				946	943		(PO ₄) ³⁻ symmetric stretching
891.7	16.9	0.5	889.3	13.4	0.9	885	890	888	(UO ₂) ²⁺ antisymmetric stretching
857.4	34.5	1.9				855	871		(AsO ₄) ³⁻

									antisymmetric stretching
						829	830		(AsO ₄) ³⁻ antisymmetric stretching
836.4	16.9	10.0	838.6	13.1	15.6				(AsO ₄) ³⁻ symmetric stretching
822.7	26.0	1.6				802	802		(UO ₂) ²⁺ symmetric stretching
795.1	6.4	0.6	796.5	8.4	6.5			796	(UO ₂) ²⁺ symmetric stretching
790.1	20.0	22.2	786.6	13.3	6.1				(AsO ₄) ³⁻ symmetric stretching
			778.7	48.6	7.4				(AsO ₄) ³⁻ symmetric stretching
770.9	28.0	8.2	771.2	11.1	1.4	779	778	778	(AsO ₄) ³⁻ symmetric stretching
			721.0	26.7	0.7				(AsO ₄) ³⁻ symmetric stretching
614.8	34.8	0.4	615.2	15.7	0.7				
			561.6	25.5	0.6	557	563	560	(PO ₄) ³⁻ bending
546.0	78.7	3.3				538	545		(PO ₄) ³⁻ bending
			516.9	10.3	19.9				
			512.4	15.6	3.2				
513.3	16.9	8.3	487.4	20.2	3.6				BiO symmetric stretch
491.4	71.4	10.5							(AsO ₄) ³⁻ bending
430.3	27.3	2.0	431.6	10.8	1.2	456	458	432	(AsO ₄) ³⁻ or (PO ₄) ³⁻ bending
397.9	29.5	3.7	390.9	25.5	1.7				(AsO ₄) ³⁻ bending
365.2	89.7	3.6	367.4	12.1	2.7				(AsO ₄) ³⁻ bending
330.0	14.9	1.6	329.1	7.9	1.5				
295.9	23.5	4.2	299.0	12.0	8.9				(UO ₂) ²⁺ bending

277.8	68.1	4.8	278.0	11.5	2.1				
239.9	14.4	0.6	239.9	12.7	1.6				
208.5	51.4	4.5	217.7	27.3	8.9				(UO ₂) ²⁺ bending
198.7	9.6	0.2	197.5	17.4	2.5				
			179.8	8.6	0.8				
154.1	12.2	1.0	152.7	4.9	0.6				

Table 4 Table of the Raman spectroscopic results at 298 and 77 K and in comparison with published infrared data of walpurgite

List of Figures

Figure 1 Raman spectra in the 650 to 950 cm^{-1} region of walpurgite at 298 and 77 K.

Figure 2 Raman spectra in the 150 to 650 cm^{-1} region of walpurgite at 298 and 77 K.

Figure 3 Raman spectra in the 3200 to 3800 cm^{-1} region of walpurgite at 298.

List of Tables

Table 1 Factor group analysis of the uranyl units

Table 2 Factor group analysis of the arsenate units

Table 2 Factor group analysis of the water units

Table 4 Table of the Raman spectroscopic results at 298 and 77 K and in comparison with published infrared data of walpurgite

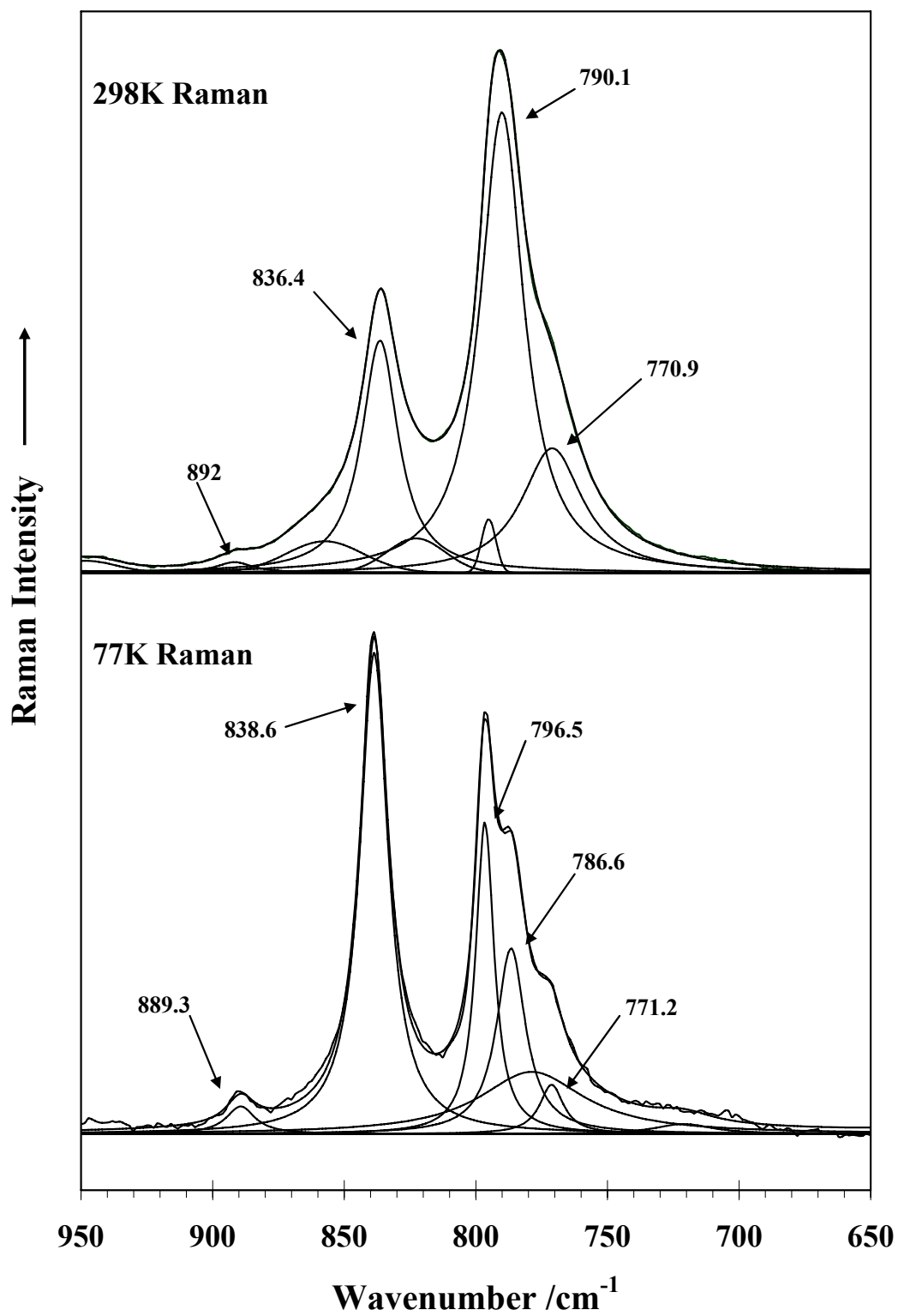


Figure 1

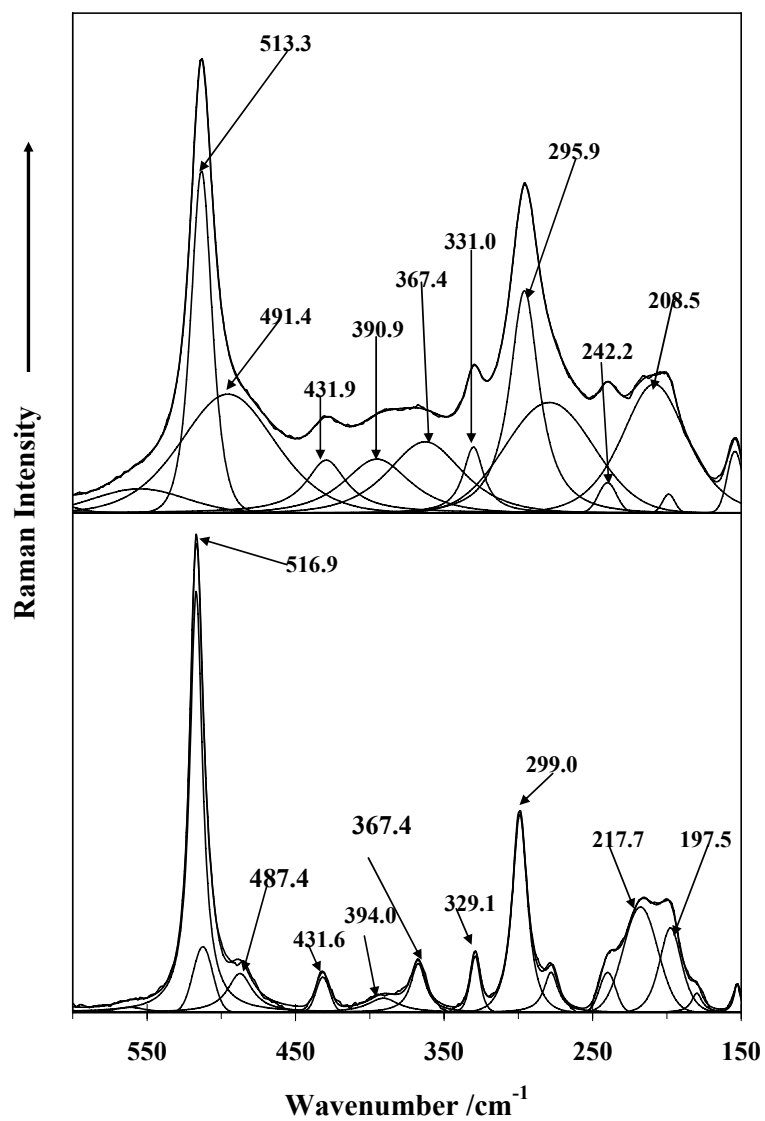


Figure 2

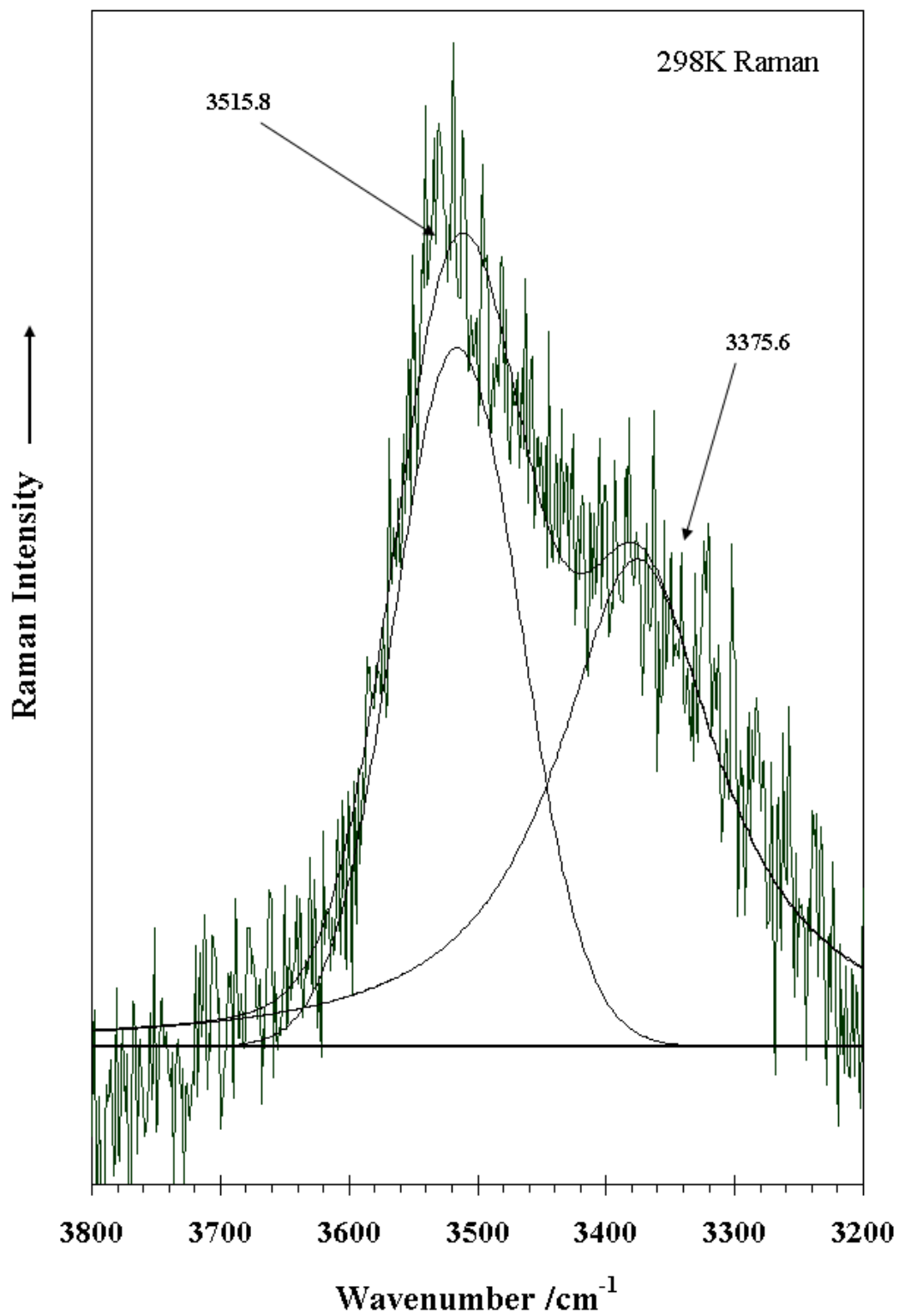


Figure 3

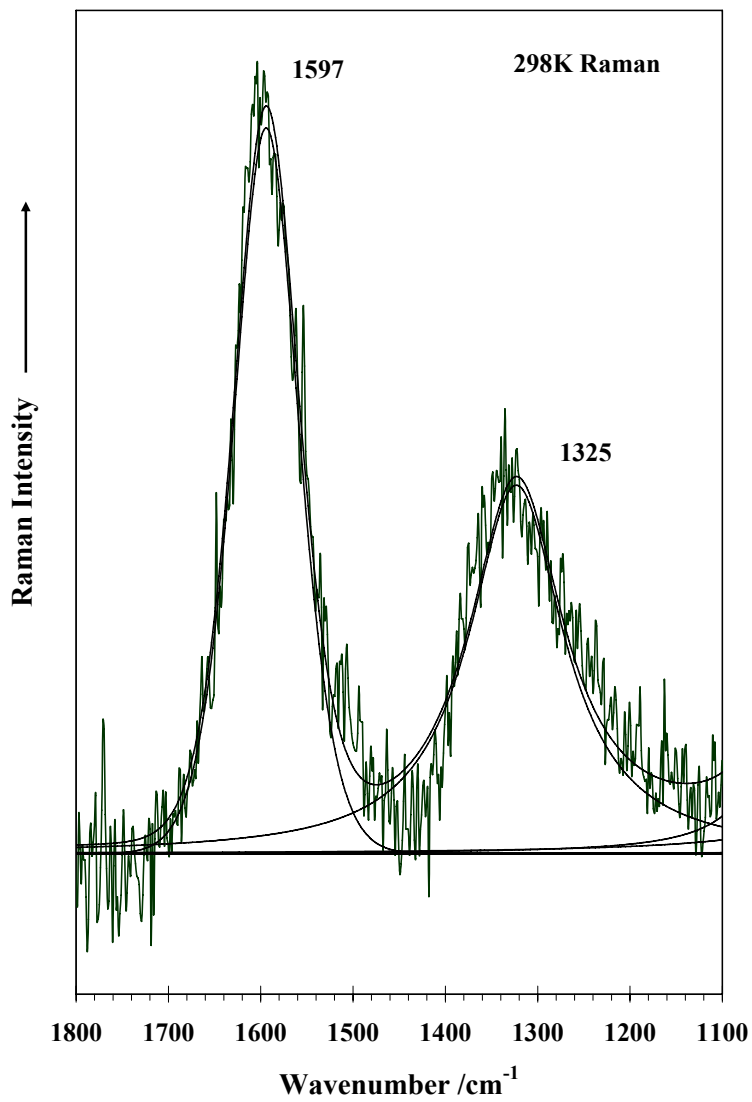


Figure 4

